Available online at www.sciencedirect.com
ScienceDirect
Journal of Power Sources 179 (2008) 351–356
JOURNAL OF POWER SOURCES
www.elsevier.com/locate/jpowsour

Short communication

Nonflammable electrolyte for 3-V lithium-ion battery with spinel materials $LiNi_{0.5}Mn_{1.5}O_4$ and $Li_4Ti_5O_{12}$

H.F. Xiang [a], Q.Y. Jin [b], R. Wang [b], C.H. Chen [b,*], X.W. Ge [a,**]

[a] *Department of Polymer Science and Engineering, University of Science and Technology of China, Anhui, Hefei 230026, PR China*
[b] *Laboratory of Advanced Functional Materials and Devices, Department of Materials Science and Engineering, University of Science and Technology of China, Anhui, Hefei 230026, PR China*

Received 18 October 2007; received in revised form 26 November 2007; accepted 28 December 2007
Available online 4 January 2008

Abstract

The compatibility between dimethyl methylphosphonate (DMMP)-based electrolyte of 1 M $LiPF_6$/EC + DMC + DMMP (1:1:2 wt.) and spinel materials $Li_4Ti_5O_{12}$ and $LiNi_{0.5}Mn_{1.5}O_4$ was reviewed, respectively. The cell performance and impedance of 3-V $LiNi_{0.5}Mn_{1.5}O_4$/$Li_4Ti_5O_{12}$ lithium-ion cell with the DMMP-based nonflammable electrolyte was compared with the baseline electrolyte of 1 M $LiPF_6$/EC + DMC (1:1 wt.). The nonflammable DMMP-based electrolyte exhibited good compatibility with spinel $Li_4Ti_5O_{12}$ anode and high-voltage $LiNi_{0.5}Mn_{1.5}O_4$ cathode, and acceptable cycling performance in the $LiNi_{0.5}Mn_{1.5}O_4$/$Li_4Ti_5O_{12}$ full-cell, except for the higher impedance than that in the baseline electrolyte. All of the results disclosed that the 3 V $LiNi_{0.5}Mn_{1.5}O_4$/$Li_4Ti_5O_{12}$ lithium-ion battery was a promising choice for the nonflammable DMMP-based electrolyte.

Keywords: Lithium-ion batteries; Nonflammable electrolyte; $Li_4Ti_5O_{12}$; $LiNi_{0.5}Mn_{1.5}O_4$

1. Introduction

Lithium-ion batteries are now widely used as energy storage devices for portable electronic devices such as laptop computers, cellular phones and digital cameras due to their high energy density. However, safety concern has become the main obstacle for the development of lithium-ion batteries for electric vehicles (EV) and hybrid electric vehicle (HEV) applications, which is greatly related to the high flammability of nonaqueous electrolyte [1,2]. So, recent efforts have been focused on finding the nonflammable electrolytes [3–9]. In our previous work [10,11], dimethyl methylphosphonate (DMMP) was considered as a promising flame-retardant additive or cosolvent, and also the DMMP-based electrolyte with a high concentration (exceeding 50 wt.%) has been validated to have the high safety characteristic. Unfortunately, the nonflammable DMMP-based electrolyte had a poor compatibility with the carbonaceous anodes, just as the trimethyl phosphate (TMP)-based nonflammable electrolyte, because both additives in the nonflammable electrolytes had similar stereo hindrances to propylene carbonate (PC) and would exert similar strains into the graphite structure and cause exfoliation [3,8,9]. Although the compatibility between the nonflammable electrolytes and the carbonaceous anodes could be improved by introducing film-formation additives, still the increased impedance from the thick solid electrolyte interface (SEI) would reduce the capacity and deteriorate the cycling performance [9,11].

The spinel $Li_4Ti_5O_{12}$ has been demonstrated as an alternative anode material because it has a very flat plateau at around 1.5 V versus Li^+/Li and displays excellent reversibility and structural stability as a zero-strain insertion material in the charge–discharge process [12]. The stable spinel structure will seldom change in the PC-containing electrolyte [13], which is different from the graphite anode with the brittle layer structure that can be easily exfoliated for co-interaction of the solvent with lithium ion. Moreover, the 1.5 V voltage plateau also can avoid the carbonate solvent, especially PC, decomposing reductively to the gaseous products. Since the reduction of the flame retar-

* Corresponding authors. Tel.: +86 551 3606971; fax: +86 551 3602940.
** Corresponding authors. Tel.: +86 551 3607410; fax: +86 551 5320512.
E-mail addresses: cchchen@ustc.edu.cn (C.H. Chen), xwge@ustc.edu.cn (X.W. Ge).

0378-7753/$ – see front matter © 2008 Elsevier B.V. All rights reserved.
doi:10.1016/j.jpowsour.2007.12.089

dant additive—DMMP occurs just at the potential below 1.2 V versus Li^+/Li [11], it is logical that the DMMP-based electrolyte would be compatible with the $Li_4Ti_5O_{12}$ anode.

To obtain an operating voltage of more than 3 V, the so-called 5 V spinel $LiNi_{0.5}Mn_{1.5}O_4$ cathode will be used to couple with the spinel $Li_4Ti_5O_{12}$ anode and fabricate the lithium-ion battery. $LiNi_{0.5}Mn_{1.5}O_4$ is one of the most promising and attractive cathodes because of its acceptable stability, good cycling performance and high-dominant potential plateau at around 4.7 V [14,15]. Compared with $LiCoO_2$, $LiNi_{0.5}Mn_{1.5}O_4$ also has the obvious advantage of low cost. By the partial substitution of Mn with Ni, the better cycling performance and higher energy density have been found for $LiNi_{0.5}Mn_{1.5}O_4$ than plain $LiMn_2O_4$, even though the spinel $LiNi_{0.5}Mn_{1.5}O_4$ has a limitation of requiring an electrolyte for the high-operating potential. Based on our previous work [10,11], DMMP has excellent anodic stability, so it is expected that DMMP-based electrolyte would have such a wide electrochemical window that it could allow a stable electrochemical performance on the high-voltage $LiNi_{0.5}Mn_{1.5}O_4$ electrode.

The objectives of this work are to examine whether or not the DMMP-based electrolyte with a high content of DMMP (50 wt.%), which could be considered as a nonflammable electrolyte with high safety characteristic, can be compatible with the spinel materials $Li_4Ti_5O_{12}$ and $LiNi_{0.5}Mn_{1.5}O_4$. Furthermore, the corresponding 3 V full-cell with the nonflammable electrolyte will also be investigated in detail, in order to find the new way to the high safety lithium-ion batteries.

2. Experimental

$Li_4Ti_5O_{12}$ was prepared by solid-state reaction method [13]. The starting materials, TiO_2-anatase and Li_2CO_3 in a Li:Ti molar ratio of 4.05:5.0 were mixed in cyclohexane and ball-milled for 48 h. Then the dried mixture was heated at 150 °C for 12 h and 800 °C for 24 h in air atmosphere to obtain white $Li_4Ti_5O_{12}$ powder. $LiNi_{0.5}Mn_{1.5}O_4$ was prepared by radiated polymer gel (RPG) method [16]. $LiNO_3$, $Ni(NO_3)_2{\bullet}6H_2O$, and $Mn(CH_3COO)_2{\bullet}4H_2O$ were dissolved in de-ionized water in the molar ratio of Li:Ni:Mn = 1.05:0.5:1.5 to obtain a 0.5 mol L^{-1} solution, then acrylic acid (AA) (CH_2=CHCOOH) was added to form an AA–H_2O (1:2, v/v) solution, the pH value of which was about 2. An excessive amount of lithium was added for the compensation of lithium evaporation during calcination. The monomer AA was polymerized under the condition of Co^{60}-ray irradiation (intensity of 35 Gy min^{-1}) for 24 h. Thus, a green polymer gel was obtained. The gel was heated at 140 °C for 8 h to get rid of the impregnated water and AA residue. The precursor obtained was then decomposed at 450 °C for 5 h in air to obtain the Li–Ni–Mn oxide powders. A subsequent heat treatment was carried out at 950 °C in air for 10 h followed by a slow cooling step (approximately 12 °C h^{-1} cooling rate) to obtain $LiNi_{0.5}Mn_{1.5}O_4$ powder.

Composite electrodes consisting of $Li_4Ti_5O_{12}$ or $LiNi_{0.5}Mn_{1.5}O_4$ (75 wt.%), acetylene black (15 wt.%) and poly(vinylidene fluoride) (PVDF) (10 wt.%) were made on aluminum and copper foils, respectively. As-purchased DMMP (Qingdao Lianmei Chemical Co., Ltd.) was purified with a distillation step under vacuum and dried before use over molecular sieves (4A). Carbonate solvents (Guotai Huarong New Chemical Materials Co.), and $LiPF_6$ (Tianjin Jinniu Power Sources Material Co.) were used as received. The electrolytes were prepared under a highly pure argon atmosphere in an argon-filled glove box (MBraun Labmaster 130). All solvent ratios indicated in this paper were in weight ratios. CR2032 coin cells were assembled in the glove box and then galvanostatically cycled on a multi-channel battery cycler (Neware BTS2300, Shenzhen). In the $Li_4Ti_5O_{12}/LiNi_{0.5}Mn_{1.5}O_4$ full-cells, the mass ratio of $Li_4Ti_5O_{12}$ and $LiNi_{0.5}Mn_{1.5}O_4$ was controlled at about 2:3, so that the cell capacity was determined by the negative electrode.

All of the cells were galvanostatically cycled at room temperature at a current of 0.2 mA cm^{-2}. For the positive and negative half-cells, the cutoff voltages were set as 3.0–5.0 V and 2.5–1.0 V, respectively. The full-cells were cycled between 2.0 V and 3.5 V at a current of 0.2 mA cm^{-2}, about C/4 rate. The electrochemical stability of the electrolytes on the electrodes was measured by cyclic voltammetry (CV) using the above coin cells at a scan rate of 0.1 mV s^{-1} on a CHI 604A Electrochemical Workstation. The ac impedance was also measured with the CHI 604A Electrochemical Workstation, with the frequency range and voltage amplitude set as 100 kHz to 0.01 Hz and 5 mV, respectively. The internal resistance of the cells was also measured by a current interruption technique. This was done by cutting off the current intermittently for 1 min through the process of charge and recording the voltage change after interruption. Thus, the dc impedance of a cell (R_{dc}) can be calculated as $R_{dc} = \Delta U/\Delta I$ [16].

3. Results and discussion

The $Li_4Ti_5O_{12}$ and $LiNi_{0.5}Mn_{1.5}O_4$ powders synthesized have been validated with a cubic spinel structure and no obvious impurity phase detected [13,16]. In order to evaluate objectively the electrochemical performance of the two spinel materials, a baseline electrolyte, i.e. 1 M $LiPF_6$/EC + DMC (1:1), is compared with the nonflammable DMMP-based electrolyte of 1 M $LiPF_6$/EC + DMC + DMMP (2:1:1). Cyclic voltammetry results of the two electrolytes on the $Li_4Ti_5O_{12}$ anode are shown in Fig. 1. In the baseline electrolyte, the reduction peak appears at about 1.38 V, which is correlated to lithium insertion and the spinel/rock-salt phase transition, and the asymmetric oxidation peak appears near 1.70 V during the reverse process (curve a). As for the DMMP-based electrolyte, the reduction peak for the first cycle occurs at the lower potential of 1.3 V and is broader than that of the baseline electrolyte. Furthermore, the more asymmetric and broader oxidation peak looks like a strong oxidation peak at 1.9 V coupled with a shoulder peak around 1.8 V at the first cycle (curve b). Nevertheless, a symmetric narrow oxidation peak can be found around 1.7 V at the second cycle (curve c). The reason of the appearance of the misshapen oxidation peak at the first cycle after the introduction of DMMP is not clear, but we still can conclude that the DMMP-based electrolyte has a good cathodic stabil-

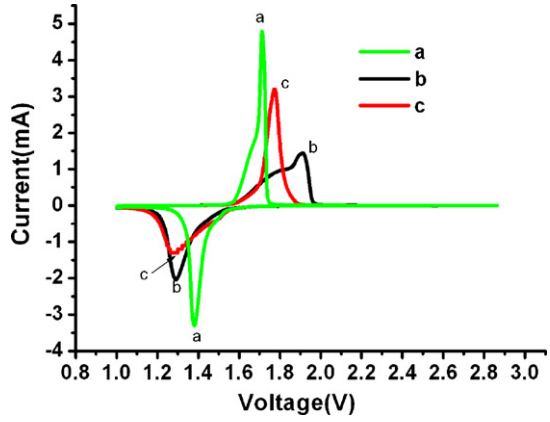

Fig. 1. Cyclic voltammograms of $Li_4Ti_5O_{12}$/Li half-cells with two kinds of electrolytes—a: 1 M $LiPF_6$/EC + DMC (1:1), b: 1 M $LiPF_6$/EC + DMC + DMMP (1:1:2) at the first cycle and c: 1 M $LiPF_6$/EC + DMC + DMMP (1:1:2) at the second cycle.

ity on the $Li_4Ti_5O_{12}$ electrode other than on the carbonaceous anodes.

Fig. 2 shows the first charge–discharge voltage profiles of $Li_4Ti_5O_{12}$/Li half-cells with the nonflammable electrolyte compared with the baseline electrolyte. It can be seen that there is no significant difference between the two kinds of electrolytes for the first charge–discharge voltage profiles, which indicates further that the nonflammable DMMP-based electrolyte is compatible with the $Li_4Ti_5O_{12}$ anode. It is worth mentioning that there is no obvious double plateaus corresponding to the two oxidation peaks (Fig. 1), perhaps because the galvanostatical charge at the constant current can overcome some kinetic effect from the greater viscosity of the DMMP-based electrolyte more easily than the non-constant current during the cyclic voltammetry test. The cycling performance of $Li_4Ti_5O_{12}$/Li half-cells with different electrolytes and ac impedance are shown in Fig. 3, from which we can find out that they both have good cycling performance although the impedance in the case of the non-

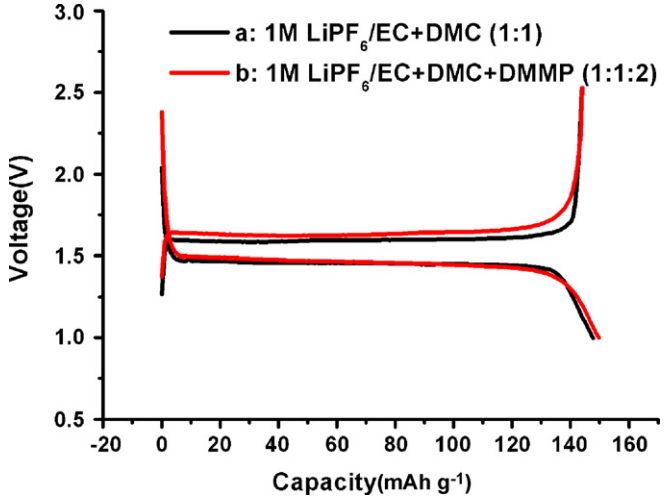

Fig. 2. The first charge–discharge voltage profiles of $Li_4Ti_5O_{12}$/Li half-cells with the baseline electrolyte (a: 1 M $LiPF_6$/EC + DMC (1:1)) and the nonflammable DMMP-based electrolyte (b: 1 M $LiPF_6$/EC + DMC + DMMP (1:1:2)).

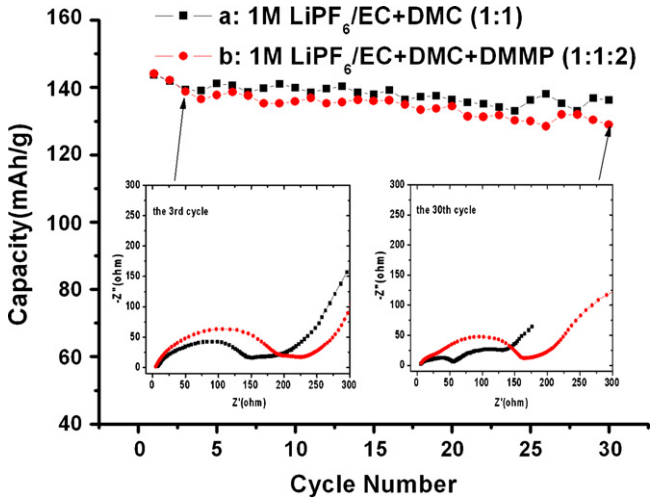

Fig. 3. The cycling performance and ac impedance of $Li_4Ti_5O_{12}$/Li half-cells with the baseline electrolyte (a: 1 M $LiPF_6$/EC + DMC (1:1)) and the nonflammable electrolyte (b: 1 M $LiPF_6$/EC + DMC + DMMP (1:1:2)). The ac impedance was measured after the cells had been discharged to 1.0 V and the cells been placed statically for about 30 min.

flammable electrolyte is slightly higher than that of the baseline electrolyte. From the results above, it can be concluded that the DMMP-based nonflammable electrolyte, which is able to destroy the graphite layer structure, has the good compatibility with the spinel $Li_4Ti_5O_{12}$ anode.

Cyclic voltammograms of the two electrolytes on the $LiNi_{0.5}Mn_{1.5}O_4$ cathode, shown in Fig. 4, indicate that it is difficult to detect the redox peaks around 4 V, related to the Mn^{3+}/Mn^{4+} couple, for the two kinds of electrolytes. But redox transition in the 5 V domain demonstrates quite reversible electrochemical behavior. Thus, the $LiNi_{0.5}Mn_{1.5}O_4$ powder synthesized exhibits the good electrochemical performance, and above all, DMMP has promising electrochemical stability in the wide electrochemical window up to 5 V. Furthermore, $LiNi_{0.5}Mn_{1.5}O_4$/Li half-cells were used to evaluate the compatibility of the nonflammable electrolyte with the 5 V

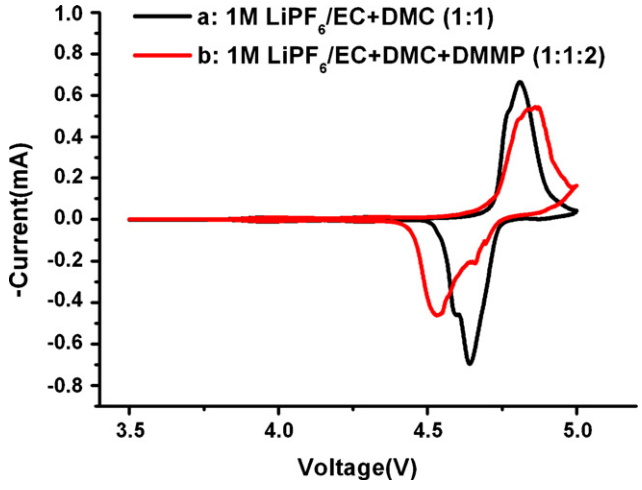

Fig. 4. Cyclic voltammograms of $LiNi_{0.5}Mn_{1.5}O_4$/Li half-cells with two kinds of electrolytes—(a: 1 M $LiPF_6$/EC + DMC (1:1) and b: 1 M $LiPF_6$/EC + DMC + DMMP (1:1:2)).

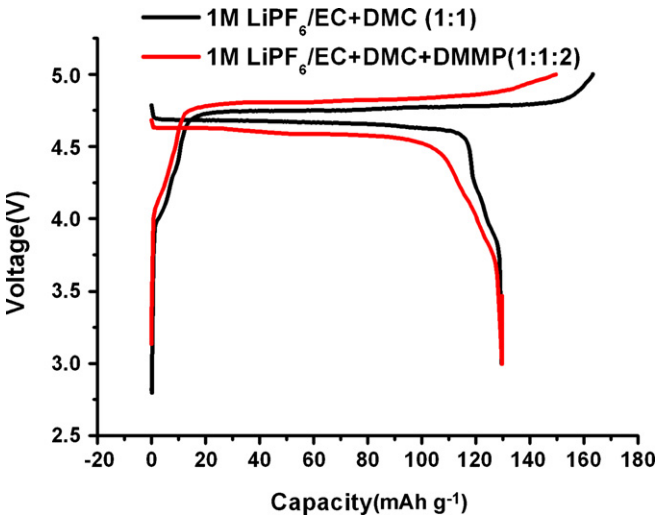

Fig. 5. The first charge–discharge voltage profiles of $LiNi_{0.5}Mn_{1.5}O_4$/Li half-cells with the baseline electrolyte (a: 1 M $LiPF_6$/EC + DMC (1:1)) and the DMMP-based electrolyte (b: 1 M $LiPF_6$/EC + DMC + DMMP (1:1:2)).

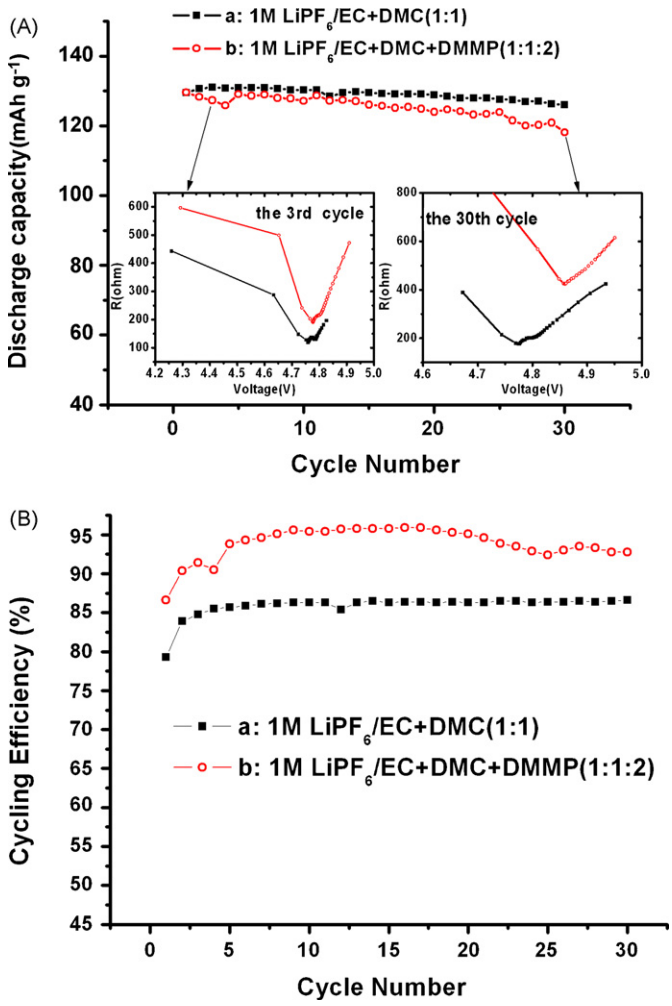

Fig. 6. The cycling performance (A) combined with dc impedance and cycling efficiency (B) of $LiNi_{0.5}Mn_{1.5}O_4$/Li half-cells with the baseline electrolyte (a: 1 M $LiPF_6$/EC + DMC (1:1)) and the DMMP-based electrolyte (b: 1 M $LiPF_6$/EC + DMC + DMMP (1:1:2)).

$LiNi_{0.5}Mn_{1.5}O_4$ cathode, as shown in Fig. 5. There seems hardly to be any difference between the nonflammable electrolyte and the baseline electrolyte in the $LiNi_{0.5}Mn_{1.5}O_4$/Li half-cells about the discharge specific capacity. However, with the introduction of a great deal DMMP, the viscosity of the nonflammable electrolyte could be increased greatly and the polarization becomes inevitable. Hence the lower discharge voltage plateau and higher charge voltage plateau appear in the case of the nonflammable electrolyte. As the irreversible capacity is concerned, the positive half-cells with the nonflammable electrolyte results in less capacity loss than the baseline electrolyte. The cycling performance of $LiNi_{0.5}Mn_{1.5}O_4$/Li half-cells with different electrolytes was compared and dc impedance was also explored, as shown in Fig. 6A. The DMMP-based electrolyte still shows acceptable cycling performance in the $LiNi_{0.5}Mn_{1.5}O_4$/Li half-cells compared with the baseline electrolyte. As the discharge capacity and capacity retention are concerned, the cell using DMMP-based electrolyte is not as excellent as the cell using the baseline electrolyte, which is apparently related to the more pronounced impedance rise in the nonflammable electrolyte. The dc impedance of the 3rd and the 30th cycles against the cell voltage is also inserted in Fig. 6A. At the third cycle, the "w"-shaped curve can be found easily for the nonflammable electrolyte as well as for the baseline electrolyte, just like our previous work [16]. Here, we also find that it is in fact a distorted "w"-shape which has a lower left minimum corresponding to the Ni^{2+}/Ni^{3+} transition and a higher right minimum corresponding to Ni^{3+}/Ni^{4+} transition. According to Ceder and coworkers [17], for the layered $LiM_{1-x}M'_xO_2$ positive electrodes, lithium diffusion is faster when the oxidation state of M is lower because lithium ions experience lower energy barrier which is mainly determined by the repulsion between Li^+ and M'^{n+}. Similarly, since the average oxidation state of the Ni^{2+}/Ni^{3+} transition is lower than that of the Ni^{3+}/Ni^{4+} transition, Li^+ transport will encounter much less repulsion and overcome a lower energy barrier on the Ni^{2+}/Ni^{3+} transition balance than on the Ni^{3+}/Ni^{4+} transition balance. As a result, the lower dc impedance of the Ni^{2+}/Ni^{3+} transition and the higher dc impedance of the Ni^{3+}/Ni^{4+} transition constitute the distorted "w"-shaped curve. In the 30th cycle, the dc impedance of the $LiNi_{0.5}Mn_{1.5}O_4$/Li half-cells with the nonflammable electrolyte becomes much higher and the "w"-shaped curve part appears at higher cell voltages, compared with the baseline electrolyte. Moreover, the curve shape becomes more like "v", especially for the nonflammable electrolyte. In short, the impedance increases more rapidly, resulting in more capacity loss of the $LiNi_{0.5}Mn_{1.5}O_4$/Li half-cells with the nonflammable electrolyte than with the baseline electrolyte. Nevertheless, as shown in Fig. 6B, the cycling efficiency of the nonflammable electrolyte is higher than that of the baseline electrolyte, which might be due to the formation of a DMMP-derived phosphate protective layer on the highly activated cathode surface at the high potential around 5 V versus Li^+/Li, just like the other similar phosphorous compound [18].

After the negative and positive half-cells have been explored, the electrochemical performance of the $LiNi_{0.5}Mn_{1.5}O_4/Li_4Ti_5O_{12}$ full-cells with the nonflammable

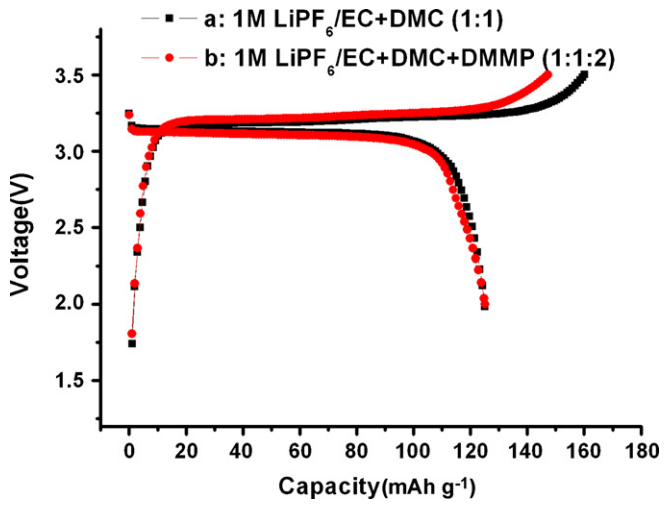

Fig. 7. The first charge–discharge voltage profiles of $LiNi_{0.5}Mn_{1.5}O_4/Li_4Ti_5O_{12}$ full-cells with the baseline electrolyte (a: 1 M $LiPF_6$/EC + DMC (1:1)) and the DMMP-based electrolyte (b: 1 M $LiPF_6$/EC + DMC + DMMP (1:1:2)).

electrolyte is compared with the baseline electrolyte. Fig. 7 shows the charge–discharge voltage profiles of the full-cells with the different electrolytes. There is no obvious difference between two kinds of electrolytes, except that the irreversible capacity shows similar relationship as the positive half-cells. The distinct polarization from the introduction of DMMP makes the charge voltage plateau shift to higher values. It could be surmised that the discrepancy about the irreversible capacity between the different electrolytes would become smaller with increasing the upper cutoff voltage. On the other hand, perhaps a passivation layer is formed mostly owing to the contribution of DMMP and less Li^+ is consumed for a lower content of EC and DMC in the DMMP-based electrolyte. Hence the columbic efficiency is higher in the case of DMMP-based electrolyte.

The cycling performance of $LiNi_{0.5}Mn_{1.5}O_4/Li_4Ti_5O_{12}$ full-cells with different electrolytes and dc impedance are shown in Fig. 8. It can be seen that the 3 V $LiNi_{0.5}Mn_{1.5}O_4/Li_4Ti_5O_{12}$ lithium-ion battery with the baseline electrolyte exhibits perfect cycling performance in the first 30 cycles with the capacity loss of 0.28% every cycle. As the nonflammable electrolyte is used to improve the safety characteristic, the cycling performance has been compromised slightly with the capacity loss of 0.61% every cycle. The dc impedance of the 3rd and the 30th cycles is also inserted in Fig. 8, which shows the similar curve as the positive half-cells. The "w"-shaped curve part appears at around 3.2 V, which is the difference between the 4.7 V plateau of the positive electrode and the 1.5 V plateau of the negative electrode. After the 30th cycle, the impedance of the cell containing the baseline electrolyte has only a small increase compared with the third cycle. However, that of the cell with the DMMP-based electrolyte increases by twofold and "w"-shaped curve part moves from ~3.25 V to ~3.30 V. Obviously, the stabilization of the cell impedance needs to be addressed in our follow-up study in order to further improve the designed lithium-ion batteries with the DMMP-based nonflammable electrolyte.

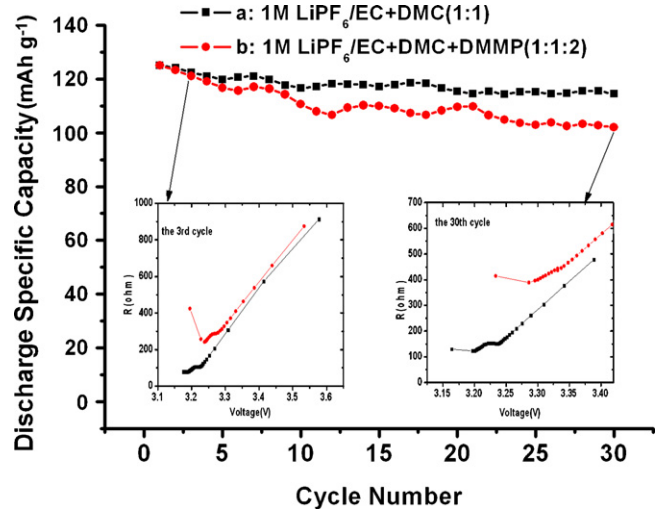

Fig. 8. The cycling performance and dc impedance of $LiNi_{0.5}Mn_{1.5}O_4/Li_4Ti_5O_{12}$ full-cells with the baseline electrolyte (a: 1 M $LiPF_6$/EC + DMC (1:1)) and the DMMP-based electrolyte (b: 1 M $LiPF_6$/EC + DMC + DMMP (1:1:2)).

4. Conclusions

The DMMP-based electrolyte that has been validated as a nonflammable electrolyte in our previous work performs good compatibility with the spinel materials $Li_4Ti_5O_{12}$ anode and $LiNi_{0.5}Mn_{1.5}O_4$ cathode. The 3 V $LiNi_{0.5}Mn_{1.5}O_4/Li_4Ti_5O_{12}$ lithium-ion cells with the DMMP-based electrolyte have an acceptable capacity loss after 30 cycles. The higher impedance of the cells with the nonflammable electrolyte is one of the important reasons for its capacity loss. Therefore, the nonflammable DMMP-based electrolyte can be used in the 3 V $LiNi_{0.5}Mn_{1.5}O_4/Li_4Ti_5O_{12}$ lithium-ion batteries, pointing to a promising way to obtain highly safe lithium-ion batteries.

Acknowledgements

This study was supported by National Science Foundation of China (grant Nos. 50372064 and 20471057).

References

[1] A.G. Ritchie, J. Power Sources 96 (2003) 1.
[2] G. Dixon, R.S. Morris, S. Dallek, J. Power Sources 138 (2004) 274.
[3] X.M. Wang, E. Yasukawa, S. Kasuya, J. Electrochem. Soc. 148 (2001) A1058.
[4] K. Xu, M.S. Ding, S. Zhang, J.L. Allen, T.R. Jow, J. Electrochem. Soc. 149 (2002) A622.
[5] K. Xu, M.S. Ding, S. Zhang, J.L. Allen, T.R. Jow, J. Electrochem. Soc. 150 (2003) A161.
[6] S. Zhang, K. Xu, T.R. Jow, J. Power Source 113 (2003) 166.
[7] Y.E. Hyung, D.R. Vissers, K. Amine, J. Power Sources 119/121 (2003) 383.
[8] X.L. Yao, S. Xie, C.H. Chen, Q.S. Wang, J.H. Sun, Y.L. Li, S.X. Lu, J. Power Sources 144 (2005) 170.
[9] X.M. Wang, C. Yamada, H. Naito, G. Segami, K. Kibe, J. Electrochem. Soc. 153 (2006) A135.
[10] H.F. Xiang, H.Y. Xu, Z.Z. Wang, C.H. Chen, J. Power Sources 173 (2007) 562.
[11] H.F. Xiang, Q.Y. Jin, C.H. Chen, X.W. Ge, S. Guo, J.H. Sun, J. Power Sources 174 (2007) 335.

[12] T. Ohzuku, A. Ueda, N. Yamamoto, J. Electrochem. Soc. 142 (1995)1431.
[13] X.L. Yao, S. Xie, C.H. Chen, Q.S. Wang, J.H. Sun, Y.L. Li, S.X. Lu, Electrochim. Acta 50 (2005) 4076.
[14] K. Amine, H. Tukamoto, H. Yasuda, Y. Fujita, J. Electrochem. Soc. 143 (1996) 1607.
[15] T. Ohzuku, S. Takeda, M. Iwanaga, J. Power Sources 81/82 (1999)90.
[16] H.Y. Xu, S. Xie, N. Ding, B.L. Liu, Y. Shang, C.H. Chen, Electrochim. Acta 51 (2006) 4352.
[17] K. Kang, Y.S. Meng, J. Breger, C.P. Grey, G. Ceder, Science 311 (2006) 977.
[18] H.Y. Xu, S. Xie, Q.Y. Wang, X.L. Yao, Q.S. Wang, C.H. Chen, Electrochim. Acta 52 (2006) 636.